第35卷 第3期 焊 接 学 报 Vol. 35 No. 3
2014年3月 TRANSACTIONS OF THE CHINA WELDING INSTITUTION March 2014

保护气体成分对双丝旁路耦合电弧 GMAW 旁路熔滴过渡形式的影响

石 玗[1,2]， 王桂龙[1,2]， 朱 明[1,2]， 樊 丁[1,2]
(1. 兰州理工大学 有色金属先进加工与再利用省部共建国家重点实验室，兰州 730050;
2. 兰州理工大学 有色金属合金及加工教育部重点实验室，兰州 730050)

摘 要: 双丝旁路耦合电弧 GMAW 的旁路焊枪选择了正极性接法即焊丝接电源负极，旁路熔滴仅依靠重力向熔池过渡，旁路熔滴尺寸较大且过渡过程并不稳定. 针对这一问题，采用已建立的双丝旁路耦合电弧焊接过程信号控制与高速摄像采集系统，采集了纯氩气保护时旁路熔滴过渡形式，并分析了旁路熔滴尺寸较大且过渡过程不稳定的原因. 在此基础上，采用 80% Ar + 20% CO_2 为保护气体进行了焊接试验. 结果表明，焊接过程中，保护气体中的 O 元素在旁路熔滴表面形成了氧化膜，旁路电弧在旁路熔滴表面的氧化膜上稳定燃烧，从而使电磁收缩力重新作用在旁路熔滴上并促进旁路熔滴向熔池过渡，因此焊接过程中旁路熔滴尺寸明显减小，熔滴过渡过程更加稳定.

关键词: 双丝旁路耦合电弧; 熔化极气体保护焊; 保护气体; 熔滴过渡
中图分类号: TG409 **文献标识码**: A **文章编号**: 0253 - 360X(2014)03 - 0015 - 04

0 序 言

双丝旁路耦合电弧熔化极气体保护焊(gas metal arc welding，GMAW)作为一种新型的高效焊接方法，通过引入旁路电弧分流了部分流经母材的电流，从而在保证高熔敷率的同时，降低了母材的热输入[1,2]. 当前国内外众多学者对双丝旁路耦合电弧 GMAW 过程的稳定性控制进行了广泛研究，文献[3]理论分析了该方法适用于高效焊接，并建立了双丝旁路耦合电弧 GMAW 耦合电弧系统的动态数学模型. 文献[4]针对双丝旁路耦合电弧 GMAW 的耦合电弧稳定性差的问题，提出了通过调节旁路弧长控制耦合电弧稳定性的方案进行了焊接试验.

双丝旁路耦合电弧 GMAW 主路采用的是反极性接法即焊丝接电源正极，旁路采用的正极性接法即焊丝接电源负极. 所以主路与旁路熔滴过渡形式并不相同. 文献[5]采用静力平衡理论，分析了旁路电弧的引入，可以促进主路熔滴向熔池过渡. 但是由于旁路焊枪选择了正极性接法，旁路熔滴尺寸较大且过渡过程并不稳定[6]. 目前对熔滴过渡形式主要采用高速摄像技术进行直观分析[7]. 文献[8]利用高速 CCD 摄像采集并分析了短路过渡 CO_2 焊接熔滴尺寸的影响因素，文献[9]搭建了高速摄像系统并采集分析了在不同保护气体下对白铜进行焊接时的熔滴过渡形式的变化规律.

文中采用快速原型技术设计了双丝旁路耦合电弧 GMAW 信号控制系统[10]，并采用被动视觉传感方式设计了高速摄像采集系统. 利用搭建的试验平台，采集了纯氩气为保护气体时双丝旁路耦合电弧 GMAW 的旁路熔滴过渡形式，并分析了旁路熔滴尺寸大、过渡形式不稳定的原因. 在此基础上提出了采用 80% Ar + 20% CO_2 为保护气体改善旁路熔滴过渡形式的方案，并进行了焊接试验.

1 双丝旁路耦合电弧 GMAW 原理

双丝旁路耦合电弧 GMAW 原理如图 1 所示. 主路焊枪与旁路焊枪分别由 GMAW 焊枪构成. 主路焊枪选用等速送丝的平特性电源并采用正极性接法即焊丝接电源负极; 旁路焊枪选用垂降特性电源并采用反极性接法即焊丝接电源正极. 熔化主路焊丝的电流在电弧弧柱区分为两部分: 一部分为流经母材的电流，另一部分为旁路电流，使得用于熔化主路焊丝的电流较高，有利于提高焊丝的熔敷率; 而通过旁路焊枪分流了部分流入母材的焊接电流，在降低了母材热输入的同时熔化旁路焊丝. 双丝旁路耦合

收稿日期: 2012 - 11 - 21
基金项目: 国家自然科学基金资助项目(51165023); 国家自然科学基金国际合作与交流资助项目(51210105024); 陇原青年创新人才扶持计划资助项目

电弧 GMAW 同时实现了高焊丝熔敷率、低母材热输入的焊接，可以适用于高速焊接、薄板焊接或低稀释率的耐磨、耐蚀材料的堆焊.

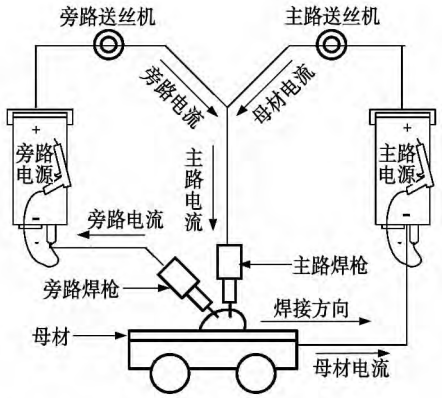

图 1 双丝旁路耦合电弧 GMAW 原理图

Fig. 1 Schematic of double-electrode gas metal arc welding

2 双丝旁路耦合电弧 GMAW 信号控制与高速摄像采集系统

双丝旁路耦合电弧 GMAW 过程控制与高速摄像采集系统如图 2 所示，其主要由信号采集与控制系统和高速摄像系统两部分组成.

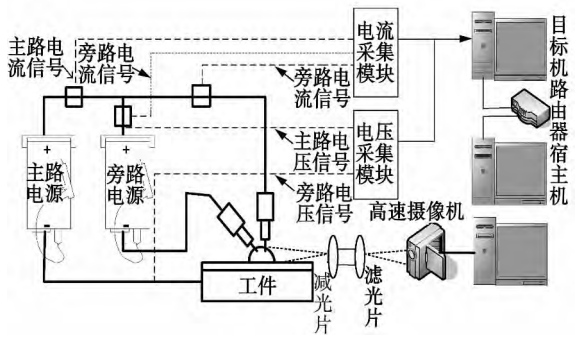

图 2 双丝旁路耦合电弧 GMAW 信号控制与高速摄像系统

Fig. 2 Signal control and speed camera system of double-electrode gas metal arc welding

为实现双丝旁路耦合 GMAW 的信号实时采集与控制，文中利用快速控制原型技术，在采用 xPC 的实时目标环境下，建立了双丝旁路耦合高效 GMAW 快速原型控制系统，能够完成对焊接过程电信号的实时采集、显示、存储及控制.

根据高速摄像视觉系统中成像光源的特性一般可分为主动式成像方式和被动式成像方式两类[10]. 由于主动式成像方式采用激光背光作为光源，传感系统的光路比较复杂且成本较高，而且双丝旁路耦合电弧 GMAW 焊接电流较大，焊接过程中电弧本身的弧光强度大，无需任何辅助光源就可使光学器件感光并记录所拍摄的图像. 所以文中采用被动式成像方式，即利用电弧本身的弧光作为光源，利用 435 nm ± 10 nm 的窄带滤光片和中性减光片的复合滤光，并采用了 GZL-CL-22C5 的 CMOS 高速摄像机、Camera Link 数据接口和 BitFlow 公司开发的 Karbon-CL 专业视频采集卡设计并建立了双丝旁路耦合电弧熔滴过渡形式高速摄像系统.

3 不同保护气体对双丝旁路耦合电弧 GMAW 旁路熔滴过渡形式的影响

为了分析双丝旁路耦合电弧 GMAW 熔滴过渡特性，采用纯氩气作为保护气体进行焊接试验，利用高速摄像系统采集了旁路熔滴过渡形式，分析了旁路熔滴过渡形式不稳定的原因. 在此基础上提出了采用 80% Ar + 20% CO_2 为保护气体改善旁路溶滴过渡形式的方案并进行了焊接试验.

焊接试验采用直径 1.6 mm 的 ER50-6 碳钢焊丝，母材为厚度 6 mm 的 Q235 钢板.

3.1 纯氩气保护时的熔滴过渡形式

采用纯氩气为保护气体进行焊接试验，焊接工艺参数如表 1 所示.

表 1 焊接工艺参数

Table 1 Welding parameters with pure argon gas as protective gas

	电弧电压 U/V	焊接电流 I/A	气体流量 q/(L·min^{-1})	焊接速度 v/(m·min^{-1})
主路	35	约 390	10	0.8
旁路	38 ~ 42	200	5	0.8

通过高速摄像系统采集到双丝旁路耦合电弧 GMAW 旁路熔滴过渡形式如图 3a 所示，其中左边电弧为主路电弧，右边为旁路电弧; 示意图如图 3b 所示.

由图 3a 可以发现，旁路熔滴尺寸较大. 由于旁路采用的是正极性接法即焊丝接电源负极，电弧会自动寻找焊丝上的氧化膜，并且由于电弧对氧化膜的破碎速度大于氧化膜自身的生成速度，所以旁路电弧爬升至焊丝固态部分，如图 3b 所示. 此时旁路电弧的电磁收缩力作用在焊丝上，对熔滴没有促进

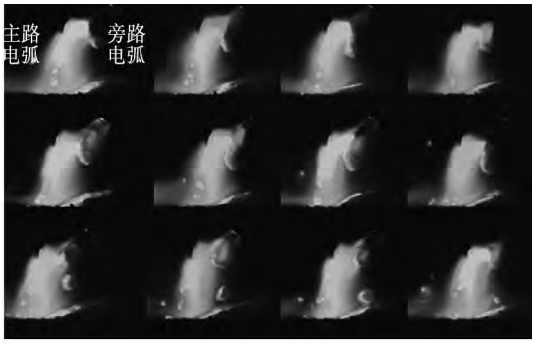

(a) 双丝旁路耦合电弧 GMAW 熔滴过渡图像

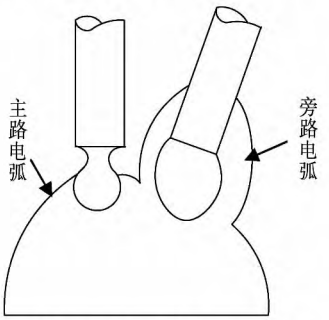

(b) 双丝旁路耦合电弧 GMAW 熔滴过渡示意图

图 3　纯氩气为保护气体时旁路熔滴过渡形式

Fig. 3　Droplet transitional forms of bypass with pure Ar gas as protective gas

作用,旁路熔滴仅在重力作用下向熔池过渡. 此时影响旁路熔滴过渡的力主要为促进熔滴过渡的熔滴重力和阻碍熔滴过渡的表面张力. 根据静力平衡理论,只有当旁路熔滴半径较大时,熔滴重力才能克服表面张力使熔滴过渡到熔池,所以旁路熔滴过渡尺寸较大. 实际焊接过程中,熔滴尺寸过大会影响焊缝质量及焊接过程稳定性.

3.2　采用 80% Ar + 20% CO_2 保护时的熔滴过渡形式

为了解决在纯氩气保护时旁路熔滴尺寸大、过渡形式不稳定的问题,提出了采用 80% Ar + 20% CO_2 混合气体为保护气体的改善方案并采用表 1 中相同的焊接工艺参数进行了焊接试验.

通过高速摄像系统采集到的 80% Ar + 20% CO_2 混合气体保护时双丝旁路耦合电弧 GMAW 熔滴过渡形式图像如图 4a 所示,其中左边电弧为主路电弧,右边为旁路电弧; 其示意图如图 4b 所示. 由图 4a 可知,和纯氩气保护时相比较,在采用 80% Ar + 20% CO_2 为保护气体时,双丝旁路耦合电弧 GMAW 旁路熔滴过渡形式发生了显著变化,旁路熔滴尺寸变小,过渡过程稳定. 由于旁路熔滴温度相对较高,保护气体中 O 元素会在熔滴表面形成氧化膜,并且旁路采用的是正极性接法,旁路电弧会自动寻找氧化膜,所以旁路电弧在旁路焊丝熔化区域内稳定燃烧,如图 4b 所示. 旁路电弧的电磁收缩力重新作用于熔滴上. 此时影响旁路熔滴过渡的力主要有促进熔滴过渡的熔滴重力、电磁收缩力和阻碍熔滴过渡的表面张力. 根据静力平衡理论,当电磁收缩力和熔滴重力大于表面张力时,熔滴脱离焊丝端部向熔池过渡. 所以和纯氩气为保护气体时相比较,采用 80% Ar + 20% CO_2 的混合气体保护时旁路熔滴尺寸减小,过渡过程稳定,并且微量的 O 元素可以改善熔池的流动性,提高了焊缝成形质量.

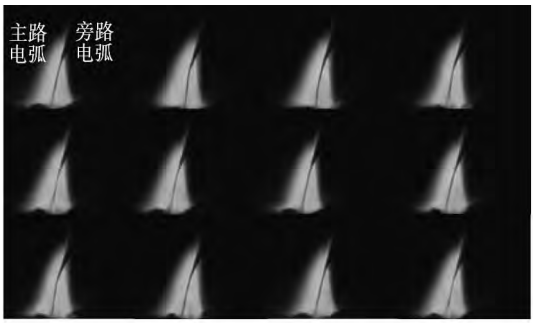

(a) 双丝旁路耦合电弧 GMAW 熔滴过渡图像

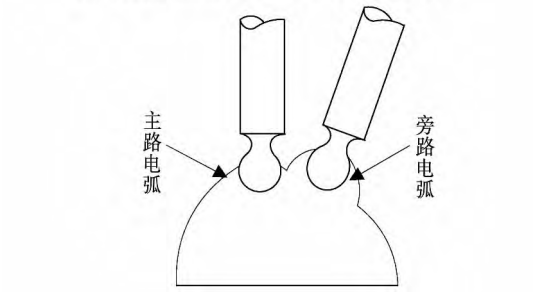

(b) 双丝旁路耦合电弧 GMAW 熔滴过渡示意图

图 4　80% Ar + 20% CO_2 混和气体保护时旁路熔滴过渡形式

Fig. 4　Droplet transitional forms of bypass with 80% Ar + 20% CO_2 mixture gas as protective gas

4　结　　论

(1) 采用纯氩气保护时,由于旁路采用了正极性接法即焊丝接电源负极,旁路电弧会在焊丝的氧化膜上燃烧,电磁收缩力没有促进旁路熔滴的过渡,旁路熔滴仅依靠重力的作用脱落. 只有当旁路熔滴半径较大时,熔滴重力才能克服表面张力使熔滴过渡到熔池.

(2) 采用 80% Ar + 20% CO_2 混合气体保护时,焊接过程中保护气体中的 O 元素会在旁路熔滴表面生成氧化膜. 旁路电弧在旁路熔滴表面的氧化膜上稳定燃烧,电磁收缩力将促进旁路熔滴脱落. 因此旁路熔滴尺寸明显减小,焊接过程更加稳定.

参考文献:

[1] Zhang Y M, Jiang M, Lu W. Double electrodes improve GMAW heat input control [J]. Welding Journal, 2004, 83(11): 39 – 41.

[2] Li K H, Chen J S, Zhang Y M. Double-electrode GMAW process and control [J]. Welding Journal, 2007, 86(8): 231 – 237.

[3] 朱 明, 石 玗, 王桂龙, 等. 双丝旁路耦合电弧高效熔化极气体保护焊双变量解耦控制模拟及试验分析 [J]. 机械工程学报, 2012, 48(22): 46 – 51.
Zhu Ming, Shi Yu, Wang Guilong, *et al*. Simulation and experiment of decoupling control for consumable DE-GMAW [J]. Journal of Mechanical Engineering, 2012, 48(22): 46 – 51.

[4] 朱 明, 石 玗, 黄健康, 等. 双丝旁路耦合电弧高效熔化极气体保护焊过程模拟及控制 [J]. 机械工程学报, 2012, 48(10): 45 – 49.
Zhu Ming, Shi Yu, Huang Jiankang, *et al*. Simulation and control of consumable DE-GMAW process [J]. Journal of Mechanical Engineering, 2012, 48(10): 45 – 49.

[5] Shi Y, Liu Y, Zhang Y. Analysis of metal transfer and correlated influences in dual-bypass GMAW of aluminum [J]. Welding Journal, 2008, 87(9): 229 – 236.

[6] 华爱兵, 殷树言, 陈树君, 等. 直流正接 MAG 焊电弧及熔滴过渡特性 [J]. 机械工程学报, 2010, 46(6): 134 – 138.
Hua Aibing, Yin Shuyan, Chen Shujun, *et al*. Arc and drop transfer behaviors of MAG welding process with direct current electrode negative [J]. Journal of Mechanical Engineering, 2010, 46(6): 134 – 138.

[7] 李 桓, 李国华, 李俊岳, 等. 熔化极电弧焊熔滴过渡过程的高速摄影 [J]. 机械工程学报, 2002, 13(9): 796 – 798.
Li Huan, Li Guohua, Li Junyue, *et al*. High-speed photography of metal transfer of electrode arc welding [J]. Journal of Mechanical Engineering, 2002, 13(9): 796 – 798.

[8] 朱志明, 吴文楷, 陈 强. 基于高速 CCD 摄像的短路过渡焊接熔滴检测与分析 [J]. 焊接学报, 2006, 27(3): 29 – 33.
Zhu Zhiming, Wu Wenkai, Cheng Qiang. Detection and analysis of the short-circuit transitional welding droplet based on the high-speed CCD camera [J]. Transactions of the China Welding Institution, 2006, 27(3): 29 – 33.

[9] 刘占民, 李明利, 薛 龙. 熔化极电弧焊熔滴过渡过程的高速摄像 [J]. 激光与红外, 2006, 36(2): 131 – 134.
Liu Zhanmin, Li Mingli, Xue Long. Slow-motion video recording for melted drop transition procedures of arc welding with consumable electrode [J]. Laser and Infrared, 2006, 36(2): 131 – 134.

[10] 石 玗, 朱 明, 黄健康, 等. 双丝旁路耦合电弧高效 MIG 焊方法及控制系统 [J]. 焊接学报, 2012, 33(3): 17 – 20.
Shi Yu, Zhu Ming, Huang Jiankang, *et al*. Study on control system for high efficiency double-electrode MIG welding [J]. Transactions of the China Welding Institution, 2012, 33(3): 17 – 20.

作者简介: 石 玗, 男, 1973 年出生, 博士, 教授, 博士研究生导师. 主要从事新型焊接方法及自动化方面的教学与科研工作. 发表论文 80 余篇. Email: shiyu@lut.cn

[上接第 14 页]

[7] 陈钟燮. 电火花表面强化工艺 [M]. 北京: 科学出版社, 2004.

[8] 汪瑞军, 李延军, 黄小鸥, 等. 电火花表面强化工艺的参数优化 [J]. 焊接, 2004(8): 21 – 24.
Wang Ruijun, Li Yanjun, Huang Xiaoou, *et al*. Parameter optimization in electric spark surface strength proces [J]. Welding & Joining, 2004(8): 21 – 24.

作者简介: 张 松, 女, 1963 年出生, 博士, 教授, 博士研究生导师. 主要研究方向为材料表面改性及激光先进制造技术. 发表论文 120 余篇. Email: songzhang_sy@163.com

MAIN TOPICS, ABSTRACTS & KEY WORDS

Microstructure of plasma sprayed composite ceramic coatings on magnalium alloy FENG Lajun[1], WANG Guanchong[1], WANG Zhaohua[2], LEI Ali[1], XU Yongzheng[1] (1. School of Materials Science and Engineering, Xi'an University of Technology, Xi'an 710048, China; 2. Materal Corrosion and Protection Laboratory of Sichuan Province, Sichuan University of Science & Engineering, Zigong 643000, China). pp 1 – 5

Abstract: In this paper, to solve the problem of poor wear resistance of magnalium alloy, the composite ceramic coating on XGFH-3 magnalium substrate was prepared by plasma spraying by using composite ceramic powder as raw materials, which were made by mechanical ball milling and PVA granulating technology. The microstructure and phase composition of the composite ceramic powders and coatings were characterized by SEM and XRD. The results show that the composite ceramic powders become remarkably flattened and homogenized with increasing milling time and new phases such as Al_3Ti and Ni_4Ti_3 are formed. However, in the spraying process, Al_3Ti and Ni_4Ti_3 intermediate phases disappear and new phases such as $MgAl_2O_4$ and Ti_5Si_3 are formed in the coating. There is elements diffusion between the substrate and the coating, resulting in strong bonding strength of the coating.

Key words: magnalium alloy; plasma spraying; mechanical alloying; reactive ceramic coatings

Analysis of dynamic arc characteristics and melt transfer behavior of AC CMT WANG Dianlong[1,2], ZHANG Zhiyang[1], LIANG Zhimin[1,2], HU Yunyan[1], WANG Jun[1,2] (1. School of Materials Science and Engineering, Hebei University of Science and Technology, Shijiazhuang 050018, China; 2. Hebei Key Laboratory of Material Near-Net Forming Technology, Hebei University of Science and Technology, Shijiazhuang 050018, China). pp 6 – 10

Abstract: In order to study the process of droplet transferring and arc behaviors of AC CMT welding, high speed photography was carried out to capture high-definition images of the arc and droplet of AC CMT welding while the electrical parameters waveforms were gathered by welding electric parameters acquisition system, and the images and waveforms were investigated simultaneously. The results show that the arc of AC CMT goes through the process of arcing-forming droplet-arc blowout. During the electrode positive period, arc concentrates at the end of filler wire and spreads on the surface of base metal, like a bell-jar. During the electrode negative period, the arc crawls up along the filler wire in a way to accelerate the melting of filler wire. Droplet transferring goes through the process of cold-hot-cold and no necking forms. During the electrode negative period the melding speed is larger, the melt transfer cycles is shorter and the diameter of droplet is larger compared with the electrode positive period.

Key words: AC CMT; arc behaviors; melt transfer; high-speed photography; data acquisition

Micro-arc spark deposition of Stellite alloy on SCH13 steel ZHANG Song[1], YI Junzhen[1], WU Chenliang[1], ZHANG Chunhua[1], WANG Mingsheng[2], XIE Yujiang[2], TAN Junzhe[3] (1. School of Materials Science and Engineering, Shenyang University of Technology, Shenyang 110870, China; 2. State Key Lab. of Corrosion and Protection, Institute of Metal Research, Chinese Academy of Sciences, Shenyang 110015, China; 3. Shenyang Blower Works Group Corporation, Shenyang 110869, China). pp 11 – 14, 18

Abstract: Stellite alloy deposition layer was prepared with micro-arc spark deposition technique on SCH13 steel. The microstructure, chemical compositions and phase structure of the deposition layers were examined by scanning electron microscopy (SEM), energy dispersive spectroscopy (EDS) and X-ray diffraction (XRD), respectively. The formation and growth mechanism of a single pulse deposition spot were studied. The results showed that the single pulse deposition spot was in splash shape. A large number of the single pulse deposition spots were superimposed continuously and then a certain thickness deposition layers were formed. The deposition layer of SCH13 steel qrowed in a column crystal style, and the deposition layer had a good metallurgical combination with the SCH3 steels. The deposition layers were consisted of γ-Co solid solution and chromium carbides, and had a low dilution rate. The microstructure of the deposition layer was slightly coarser with the increasing of the processing voltage. The average hardness of the deposition layers increased significantly compared to that of the Stellite alloy electrode.

Key words: SCH13 steel; micro-arc spark deposition; Stellite alloy; directional epitaxial growth

Effects of different protective gas on bypass metal transfer in consumable double-electrode gas metal arc welding process SHI Yu[1,2], WANG Guilong[1,2], ZHU Ming[1,2], FAN Ding[1,2] (1. Key Lab. of Non-ferrous Metal Alloys, the Ministry of Education, Lanzhou University of Technology, Lanzhou 730050, China; 2. State Key Lab. of Gansu Advanced Non-ferrous Metal Materials, Lanzhou University of Technology, Lanzhou 730050, China). pp 15 – 18

Abstract: In consumable double-electrode gas metal arc welding process, since the bypass welding wire is connected to the negative electrode of the welding power supply, only gravity promotes the bypass droplet transfer to the weld pool by using pure argon as protective gas. So the size of the bypass droplet is large and the metal transfer process is unstable. A high-speed camera acquisition system and a welding control system of the consumable double-electrode gas metal arc welding have been built to collect and analyze the bypass metal transfer process. On

this basis, a welding test was carried out by using the 80% Ar + 20% CO_2 mixture gas as protective gas. The results showed that the bypass arc burned stably on the oxide film of bypass droplet formed by CO_2 in protective gas, so the electromagnetic force and the gravity promoted the bypass metal transfer together and the size of the bypass droplet was significantly reduced.

Key words: gas metal arc welding; protective gas; metal transfer

Investigation on coupling arc electrode GPCA-TIG welding process HUANG Yong[1,2], HAO Yanzhao[2], LIU Ruilin[2] (1. State Key Laboratory of Gansu Advanced Non-ferrous Metal Materials, Lanzhou University of Technology, Lanzhou 730050, China; 2. Key Laboratory of Non-ferrous Metal Alloys and Processing, The Ministry of Education, Lanzhou University of Technology, Lanzhou 730050, China). pp 19 - 22

Abstract: A new method named coupling arc electrode GPCA-TIG welding is proposed, which combines coupling arc electrode and GPCA welding method, and with which deep penetration and high-speed welding can be achieved. In this paper, the weld surface appearances and weld cross-section shapes with traditional TIG, coupling arc electrode TIG and coupling arc electrode GPCA-TIG welding are studied. It is found that in the coupling arc electrode GPCA-TIG welding, the weld undercut and humping bead can be avoided, and meanwhile the weld depth increase. The results of the coupling arc electrode GPCA-TIG process shows that the weld depth and width increase with the decreasing of weld speed and the rising of outer nozzle position; with the increasing of arc length and flow rate of the outer gas O_2, the weld depth and width firstly increase and then decrease. The weld undercut is weaken with the increasing of welding speed, arc length and flow rate of the outer gas O_2. A good weld surface appearance can always be obtained with any outer nozzle position.

Key words: coupling arc electrode; GPCA welding; weld shape; weld undercut; humping bead

Digital control of capacitance charge-discharge pulse in electro-spark deposition power supply HAN hongbiao, LI Xiangyang (School of Mechatronics Engineering, Henan University of Science and Technology, Luoyang 471003, China). pp 23 - 26, 70

Abstract: The discharge voltage of traditional depositing power supply cannot be continuously adjusted, which limits the application range of electro-spark deposition and the efficiency of electro-spark deposition. In order to overcome this shortage, a digital control of capacitance charge-discharge pulse in electro-spark deposition power supply was developed. This power supply consists of CPU, rectifier and filter circuit, charge and its drive circuit, charge voltage comparison circuit, discharge and its drive circuit, motorial electrode, etc. With alternate charge and discharge process of this power supply, discharge voltage and discharge energy as well as discharge frequency can be adjusted steplessly. Experimental results show that the SCR of this power supply can be shut off safely when a short circuit occurs between the electrode and the workpiece, which greatly improves the efficiency of pulse output. The adjustment of discharge parameters is convenient, thus the power supply meets the requirements of various process condition.

Key words: electro-spark deposition; digital control; voltage regulation

Synthesis and characterization of carbon nanotubes reinforced TiNi composite solder QI Junlei, WAN Yuhan, ZHANG Lixia, FENG Jicai (State Key Laboratory of Advanced Welding and Joining, Harbin Institute of Technology, Harbin 150001, China). pp 27 - 30

Abstract: Low temperature PECVD method was employed for in-situ preparation of CNTs reinforced TiNi composite brazing powder on Ni-TiH2 base material, in order to solve the problems such as poor dispersity of CNTs, poor structural integrity and reaction of C and Ti. The composite brazing powder was characterized by XRD, SEM, Raman and TEM. Analysis shows that the low temperature PECVD method has not only guaranteed the structural integrity and uniform dispersity of CNTs, but also inhibited the decomposition of TiH2 at high temperatures and further inhibited the reaction between C and Ti, which realized the reinforcement of CNTs to TiNi brazing powder. The reinforcement of CNTs could release the residual stress in brazed joints, improve the properties of the joints and further achieve the reliable joining and high-temperature application of ceramic, composites and metal.

Key words: carbon nano tube; composite material; low temperature preparation; soldered seam

Plasticity and creep performance of low-Ag SnAgCuBi-xNi/Cu solder joint YANG Miaosen, SUN Fenglian, ZOU Pengfei (School of Materials Science Engineering, Harbin University of Science and Technology, Harbin 150040, China). pp 31 - 34

Abstract: In order to study the effect of Ni on plasticity and creep performance of low-Ag SnAgCuBi-xNi/Cu (x = 0, 0.05, 0.1, 0.15, 0.2) solder joint, the indentation work and indentation creep were measured and analyzed by nanoindentation method. The results show that adding Ni could improve the hardness of solder joint. Adding amounts of 0.05% and 0.1% Ni is helpful to improve the plasticity performance but produce almost no impacts on creep. A further Ni adding amount (0.15% and 0.2%) can improve the creep resistance at the expense of plasticity. It is found that Ni can improve high temperature stability of SnAgCuBi/Cu solder joints. The creep resisting performance of the solder joints is improved with Ni element increasing after 400 h aging at 150 ℃. The hardness of solder joints is improved with the Ni addition. The plasticity performance of solder joints with 0.1% Ni content is better than others.

Key words: nanoindentation; plasticity; creep; hardness

Finite element analysis of shot peening treatment to improve welding pesidual stress of 7A52 aluminum alloy HUANG Zhiye, CHEN Furong (College of Materials Science and Engineering, Inner Mongolia University of Technology, Hohhot 010051, China). pp 35 - 40